Synaptic P-Rex1 signaling regulates hippocampal long-term depression and autism-like social behavior

Jun Li[a,b,c], Anping Chai[d,e,f], Lifang Wang[a,b,c], Yuanlin Ma[a,b,c], Zhiliu Wu[a,b,c], Hao Yu[a,b,c], Liwei Mei[a,b,c], Lin Lu[a,b,c], Chen Zhang[g,h], Weihua Yue[a,b,c], Lin Xu[d,e,f,1], Yi Rao[g,h,i], and Dai Zhang[a,b,c,h,i,j,1]

[a]Institute of Mental Health, Sixth Hospital of Peking University, Beijing 100191, China; [b]National Clinical Research Center for Mental Disorders, Ministry of Health (Peking University), Beijing 100191, China; [c]Key Laboratory for Mental Health, Ministry of Health (Peking University), Beijing 100191, China; [d]Key Laboratory of Animal Models and Human Disease Mechanisms, Kunming Institute of Zoology, Chinese Academy of Sciences, Kunming 650223, Yunnan, China; [e]Kunming Institute of Zoology/The Chinese University of Hong Kong Joint Laboratory of Bioresources and Molecular Research in Common Disease, Kunming Institute of Zoology, Chinese Academy of Sciences, Kunming 650223, Yunnan, China; [f]Laboratory of Learning and Memory, Kunming Institute of Zoology, Chinese Academy of Sciences, Kunming 650223, Yunnan, China; [g]School of Life Sciences, Peking University, Beijing 100871, China; [h]Peking University-International Data Group/McGovern Institute for Brain Research, Peking University, Beijing 100871, China; [i]Peking-Tsinghua Center for Life Sciences, Peking University, Beijing 100871, China; and [j]Shenzhen Key Laboratory for Neuronal Structural Biology, Shenzhen Peking University-Hong Kong University of Science and Technology Medical Center, Shenzhen, 518035, China

Edited by Thomas C. Südhof, Stanford University School of Medicine, Stanford, CA, and approved October 27, 2015 (received for review June 30, 2015)

Autism spectrum disorders (ASDs) are a group of highly inheritable mental disorders associated with synaptic dysfunction, but the underlying cellular and molecular mechanisms remain to be clarified. Here we report that autism in Chinese Han population is associated with genetic variations and copy number deletion of P-Rex1 (phosphatidylinositol-3,4,5-trisphosphate-dependent Rac exchange factor 1). Genetic deletion or knockdown of P-Rex1 in the CA1 region of the hippocampus in mice resulted in autism-like social behavior that was specifically linked to the defect of long-term depression (LTD) in the CA1 region through alteration of AMPA receptor endocytosis mediated by the postsynaptic PP1α (protein phosphase 1α)–P-Rex1–Rac1 (Ras-related C3 botulinum toxin substrate 1) signaling pathway. Rescue of the LTD in the CA1 region markedly alleviated autism-like social behavior. Together, our findings suggest a vital role of P-Rex1 signaling in CA1 LTD that is critical for social behavior and cognitive function and offer new insight into the etiology of ASDs.

autism | social recognition | P-Rex1 | long-term depression | AMPA receptor endocytosis

Deficits in social interaction and communication skills and repetitive behavior/restricted interests have been demonstrated in people diagnosed with autism spectrum disorders (ASDs) (1). Several studies have documented impairments of social recognition [e.g., such as deficits in recognizing unfamiliar faces (2)] and in behavioral flexibility [e.g., impaired reversal learning and difficulties in error correction (3, 4)] in autistic people. However, the neurobiological mechanism responsible for the symptoms of ASDs, and especially for the deficit in social recognition, is little known.

Recent genetic studies have identified a large number of candidate genes for ASDs (5, 6), including many that code for synaptic proteins. Synaptic dysfunction may play a critical role in ASDs (7).

Here we have identified a new autism-associated gene, *Prex1*, that codes for P-Rex1 (phosphatidylinositol-3,4,5-trisphosphate-dependent Rac exchange factor 1), a Rac-specific Rho GTPase guanine nucleotide exchange factor (GEF). This gene is known to be highly expressed in neutrophils and in the mouse brain (8). Mice with the *Prex1* gene deleted ($Prex1^{-/-}$) exhibited Rac-dependent mild neutrophilia (9) and melanoblast migration defects (10). P-Rex1 influences neuronal cell motility (11) and neurite elongation (12) by regulating actin dynamics specifically at the growth cone. However, the role of P-Rex1 in regulating synaptic function and related behaviors remains unknown.

In addition to identifying an association between *PREX1* and autism in humans, we demonstrate that genetic disruption of P-Rex1 in mice leads to autism-like social behavior and to other features known to be associated with ASDs. Electrophysiological studies revealed a specific impairment of NMDA receptor (NMDAR)-dependent long-term depression (LTD) at Schaffer collateral–*cornus ammonis* region 1 (SC–CA1) synapses. Furthermore, these defects were associated with dysfunction in NMDA-induced AMPA receptor (AMPAR) endocytosis, because of defective PP1α (serine/threonine protein phosphase 1α)–P-Rex1–Rac1 (Ras-related C3 botulinum toxin substrate 1) signaling, and correcting the latter rectified the social recognition deficit of $Prex1^{-/-}$ mice. Thus, we have elucidated a synaptic mechanism underlying the deficit in social recognition induced by P-Rex1 disruption and the cognitive dysfunction associated with ASDs.

Results

Association of *PREX1* with Autism and Its Copy Number Deletion in Autistic People. We analyzed 17 tag SNPs that could capture 70.5% of the common variations in *PREX1*. The allele frequencies and results of the family-based association test (FBAT) for single-SNP analysis are shown in Table S1. Six SNPs (rs6066779, rs3934721, rs4076292, rs4810845, rs4455220, and rs6066835) showed a preferential transmission after Bonferroni correction. Pairwise linkage disequilibrium (LD) analysis identified four LD blocks (Fig. 1*A*). The specific and global haplotype tests of association in the FABT are shown in Table S2. After permutation correction, 18 haplotypes in block 1, 3 haplotypes in block 2, and 1 haplotype in block 3 displayed either significant excess transmission ($Z > 0$) or under transmission ($Z < 0$).

Significance

Impairments in social behavior and behavioral flexibility have been found in autistic people. However, the genetic mechanism that may contribute to these symptoms is unknown. Here we identified a previously unreported autism-associated gene that regulates synaptic plasticity. The mice lacking this gene exhibit deficits in AMPA receptor endocytosis and synaptic depression because of the blockade of a postsynaptic signaling pathway, leading to autism-like social recognition deficit and behavioral inflexibility. These findings provide new insights into the mechanisms underlying social recognition behavior and suggest that the synaptic depression-related signaling pathway might represent a new therapeutic target for treatment of social recognition deficit disorders such as autism spectrum disorders.

Author contributions: J.L., A.C., L.X., and D.Z. designed research; J.L., A.C., L.W., Y.M., Z.W., and L.M. performed research; L.L., C.Z., and Y.R. contributed new reagents/analytic tools; J.L., A.C., L.W., H.Y., and W.Y. analyzed data; and J.L., A.C., L.X., and D.Z. wrote the paper.

The authors declare no conflict of interest.

This article is a PNAS Direct Submission.

[1]To whom correspondence may be addressed: Email: daizhang@bjmu.edu.cn or lxu@vip.163.com

This article contains supporting information online at www.pnas.org/lookup/suppl/doi:10.1073/pnas.1512913112/-/DCSupplemental.

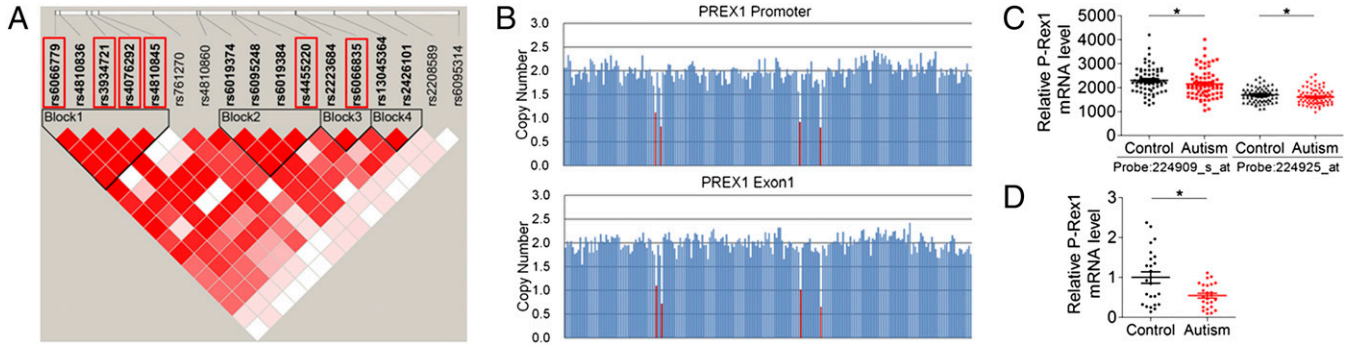

Fig. 1. The genetic association and the association of the down-regulated expression of P-Rex1 with autism in the Chinese Han population. (*A*) The LD structure of the region of *PREX1* in 239 trios according to Haploview (solid spine of LD, D' >0.8). Markers with LD [D' <1 and log of the odds (LOD) >2] are shown in red through pink with color intensity decreasing with decreasing D' value. Regions of low LD and low LOD scores (D' <1 and LOD <2) are shown in white. Variant alleles at six SNPs showed preferential transmission after Bonferroni correction (boxed in red). (*B*) Assays of copy number variation in the *PREX1* gene. The copy number states of *PREX1* promoter (*Upper*) and *PREX1* exon 1 (*Lower*) in 220 autistic people are shown. Each column indicates a patient. Four autism cases showed one copy of *PREX1* (red bars); others showed two copies (blue bars). (*C* and *D*) The *PREX1* mRNA level was decreased significantly in peripheral blood cells of autistic children as compared with healthy controls from the GEO profile database (control n = 69, autism n = 77) (*C*) and in our samples (control n = 24, autism n = 25) (*D*). *P < 0.05 by Mann–Whitney u test. Data are presented as mean ± SEM.

A copy number deletion of an approximate 1.4-kb region containing the *PREX1* promoter and exon 1 was found in 4 of 220 autistic people (Fig. 1*B*) but was not detected in 291 unrelated healthy controls (Fig. S1). In addition, the level of *PREX1* mRNA was significantly lower in the peripheral blood cells of autistic children than in those of healthy individuals in the Gene Expression Omnibus (GEO) profile database (Fig. 1*C*) (13) and in our study (Fig. 1*D*). These findings suggest that the gene dosage of *PREX1* might be down-regulated in autism.

***Prex1*$^{-/-}$ Mice Exhibit Autism-Like Behaviors.** As expected, P-Rex1 was completely absent in the brain of homozygous mutant mice (Fig. S2*A*). We tested the potential effect of the absence of P-Rex1 on behaviors related to autism (14). First, we used a three-chamber social interaction assay (15) to investigate animals' voluntary initiation of social interaction and their ability to discriminate social novelty (Fig. 2*A*). In the initial trial, *Prex1*$^{-/-}$ mice displayed normal sociability (Fig. 2 *B* and *C*). However, in the subsequent social novelty trial, WT mice displayed a preference for the novel animal (stranger 2), whereas *Prex1*$^{-/-}$ mice spent almost identical amounts of time interacting with stranger 1 and with stranger 2 (Fig. 2 *D* and *E*). Because *Prex1*$^{-/-}$ mice showed a normal interest in novelty in the novel-object recognition assay (Fig. S3*A*), we tested WT and *Prex1*$^{-/-}$ mice for social novelty recognition using a stranger mouse and their familiar cohoused WT littermate (Fig. 2*F*) (16). We found that both genotypes demonstrated a significant preference for the novel animal (Fig. 2 *G* and *H*). This result indicated that *Prex1*$^{-/-}$ mice showed selective impairment of social novelty recognition between stranger 1 and stranger 2.

Abnormal social novelty recognition usually results from a deficit in social memory (17, 18). We used a modified four-trial social memory assay (16, 19) to explore whether *Prex1*$^{-/-}$ mice showed impaired social learning and memory in re-recognizing the first stranger (stranger 1) (Fig. 2*I*). We found that the WT mice displayed normal social memory, as demonstrated by a marked habituation (decreased close interaction) to a stimulus mouse (stranger 1) during the first three trials and a striking dishabituation (increased close interaction) upon the presentation of a novel animal (stranger 2) in the fourth trial. In contrast, *Prex1*$^{-/-}$ mice showed no significant habituation to the stimulus mouse or dishabituation to the novel mouse (Fig. 2*J*), thus confirming that P-Rex1 is necessary for social memory of a stranger mouse (stranger 1).

Because olfaction is crucial for normal social behaviors in mice, we confirmed that odor recognition was normal in *Prex1*$^{-/-}$ mice by using an olfaction test (Fig. S3*B*) and an olfactory habituation/dishabituation test (Fig. S3*C*). We therefore concluded that social memory of a familiar individual (littermate) was normal in *Prex1*$^{-/-}$ mice and that the deficit in social novelty recognition between stranger 1 and stranger 2 was caused by the impaired social learning and memory of stranger 1, demonstrating that social learning and memory of a stranger mouse were deficient in *Prex1*$^{-/-}$ mice.

Isolation-induced ultrasonic vocalizations (USVs) are an infant–mother vocal communicative behavior that is thought to be relevant to autism (14, 20). We found that *Prex1*$^{-/-}$ pups emitted significantly fewer ultrasonic calls than did WT littermates (Fig. 2*K*), indicating the abnormality of social communication in *Prex1*$^{-/-}$ mice.

We evaluated spatial learning and memory by using the Morris water maze (MWM) test. *Prex1*$^{-/-}$ and WT mice showed similar learning curves (Fig. 3*A*) and probe performance (Fig. 3*B*). To assess behavioral flexibility, we first performed a classic reversal learning task using the MWM test. We found that *Prex1*$^{-/-}$ mice showed impairment in learning the new platform location (Fig. 3*C*) and spent equivalent amounts of time in the new target and opposite quadrants (Fig. 3*D*). There was no difference between the two genotypes in latency in locating a visible platform (Fig. 3*E*). To study behavioral inflexibility in more detail, we examined contextual fear extinction. *Prex1*$^{-/-}$ mice showed normal acquisition curves (Fig. 3*F*) similar to those of WT mice but a smaller reduction in freezing time during the extinction phase (Fig. 3*G*), confirming the behavioral inflexibility observed in reversal task on the MWM test. However, we found WT and *Prex1*$^{-/-}$ mice did not differ significantly in the delayed nonmatch to place T-maze task (Fig. S3*D*). Repetitive behaviors also encompass motor stereotypes, and both tend to co-occur in autistic children. We found that *Prex1*$^{-/-}$ mice spent significantly more time grooming themselves than did WT mice but showed normal jumping and digging behaviors (Fig. 3*H*).

Prex1$^{-/-}$ mice weighed slightly less than WT mice at age 12 and 16 wk (Fig. S3*E*) (9). Although the motor behavior of *Prex1*$^{-/-}$/*Prex2*$^{-/-}$ double-knockout mice is more impaired than that of *Prex2*$^{-/-}$ mice (21), *Prex1*$^{-/-}$ mice displayed normal motor coordination and balance with the rotarod (Fig. S3*F*) and normal locomotor activity in an open field test (Fig. S3 *G* and *H*). *Prex1*$^{-/-}$ mice did not show any anxiety-like behaviors (Fig. S3 *I*–*K*). To characterize sensory deficits, we measured the degree of prepulse inhibition and found no significant differences between genotypes (Fig. S3*L*).

Down-Regulation of P-Rex1–Rac1 Signaling in the CA1 Region of the Hippocampus Impairs Social Recognition Behavior. Social recognition (16, 22) and behavioral flexibility (23–25) have been shown to

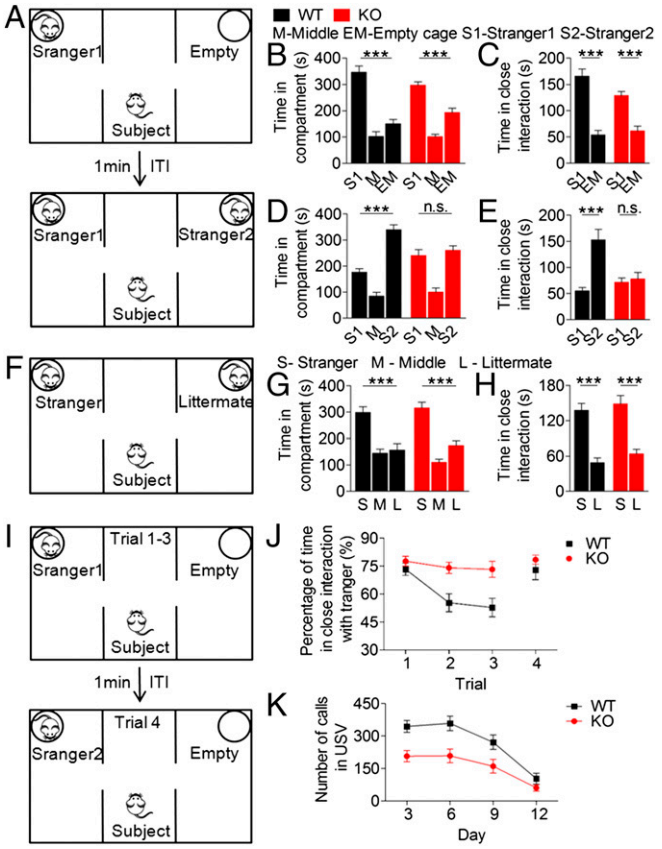

Fig. 2. *Prex1*$^{-/-}$ mice exhibit deficits in social recognition and abnormal social communication. (*A*) Schematic representation of the sociability and social novelty preference trials (n = 10 WT mice; n = 11 KO mice). ITI, intertrial interval. (*B* and *C*) In the sociability trial (stranger 1 versus empty chamber), both WT and KO mice spent more time in the chamber containing the social partner (stranger 1) (*B*) and in close interaction with stranger 1 (*C*). (*D* and *E*) In the social novelty preference trial (stranger 1 versus stranger 2), KO mice did not display a preference for the novel social partner (stranger 2). (*F*) Representative paradigm of the stranger versus littermate trial. (*G* and *H*) Both WT and KO mice spent more time in the chamber containing the novel animal (stranger) (*G*) and preferred the novel animal to a littermate (*H*). (*I* and *J*) Abnormal social recognition memory in KO mice (n = 10 mice per genotype). (*I*) Representative protocol of the four-trial social memory assay. (*J*) WT but not KO mice habituated to the same mouse (trials 1–3) and dishabituated to a novel mouse (trial 4). The groups differed significantly (n = 10 mice per genotype). (*K*) Impaired social communication by USVs in KO pups (n = WT 30 mice; n = 31 KO mice). ***P < 0.001 (two-tailed Student's t-test or two-way ANOVA). n.s., no significance. Data are presented as mean ± SEM.

depend on hippocampal function. By using in situ hybridization (ISH), we found high expression of *Prex1* mRNA in the CA1 region of the hippocampus (Fig. S2*B*), consistent with a previous report (11). Additionally, we verified the expression of P-Rex1 protein across the postnatal development of the cortex and hippocampus and the development of primary hippocampal neurons in vitro (Fig. S2 *C*–*F*). To characterize the P-Rex1^{+} cell types, double-labeling was performed; P-Rex1 protein was detected in calmodulin-dependent protein kinase II (CaMKII)-positive excitatory neurons but not in GFAP^{+} astrocytes (Fig. S2*G*).

We found no significant difference between 6-wk-old WT and *Prex1*$^{-/-}$ mice in the quantity and distribution of cortical and hippocampal neurons (Fig. S4 *A*–*N*) or in the complexity of the dendrites in the neurons of the CA1 region (Fig. S4 *O*–*S*). Then we explored the possibility of a relationship between P-Rex1 deficiency in the CA1 region and impaired social recognition behavior in adolescent mice. We acutely down-regulated *Prex1* expression in the neurons of the CA1 region in postnatal day 21 WT mice (Fig. 4 *A* and *B*). Three weeks after lentivirus (LV)-mediated shRNA injections, we performed a three-chamber social interaction test. As with *Prex1*$^{-/-}$ mice, we found that mice injected with *Prex1* shRNA, but not those injected with saline or control shRNA, showed a deficit in social recognition (Fig. 4 *C* and *D*). This result indicated that social recognition in *Prex1*$^{-/-}$ mice may result from the deletion of P-Rex1 in the CA1 region. P-Rex1 knockdown also led to a mild deficit in behavioral flexibility but not to repetitive grooming (Fig. 5 *A*–*G*).

Previous study reported that P-Rex1 regulates the activation level of Rac family members in peripheral neutrophils (8, 9). Therefore, we investigated whether abnormal activation of Rac1, which is highly expressed in the hippocampus, is involved in the social recognition deficit in *Prex1*$^{-/-}$mice. First, we found that the activation level of Rac1 (GTP-Rac1/total Rac1), but not that of Cdc42 or RhoA (Ras homolog gene family, member A), was significantly reduced in *Prex1*$^{-/-}$ hippocampi (Fig. 4 *E* and *F*). Then we injected NSC23766, a Rac1 inhibitor, into the CA1 region

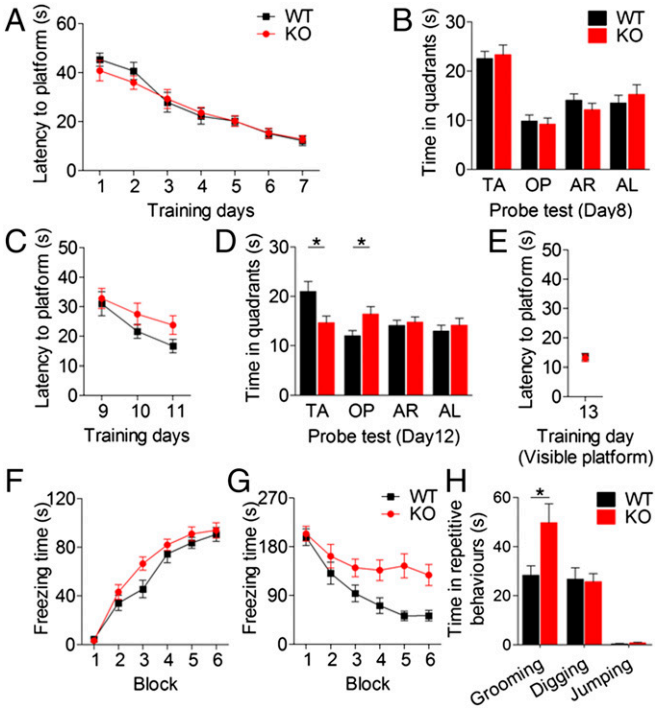

Fig. 3. *Prex1*$^{-/-}$ mice showed behavioral abnormalities in reversal learning in the MWM and fear extinction and displayed repetitive grooming. (*A*–*E*) The MWM test. (*A*) Latency to locate a hidden platform decreased significantly for both WT and KO mice over training days. (*B*) Probe test. Note that both genotypes spent significantly more time in the target quadrant. AL, adjacent left quadrant; AR, adjacent right quadrant; OP, opposite quadrant; TA, target quadrant. (*C*) *Prex1*$^{-/-}$ mice showed impairment in learning the new location of the platform in reversal training (the platform was moved to the opposite quadrant). (*D*) Reversal probe test. Note that WT mice, but not *Prex1*$^{-/-}$mice, spent significantly more time in the new target quadrant. (*E*) Genotypes did not differ in latency to locate a visible platform (n = 13 mice per genotype). *P < 0.05. (*F* and *G*) Learning and extinction of contextual fear memory. (*F*) In both genotypes freezing time increased significantly after one unconditional stimulus per block in a 12-min learning period consisting of six 2-min blocks. (*G*) Freezing time decreased more significantly in WT than in KO mice during the extinction period 24 h after learning (n = 20 WT mice; n = 19 KO mice). (*H*) Excessive stereotypical grooming in *Prex1*$^{-/-}$ mice (n = 15 mice per genotype). *P < 0.05 (two-tailed Student's t-test or repeated-measures two-way ANOVA with genotype and treatment as independent variables). n.s., no significance. Data are presented as mean ± SEM.

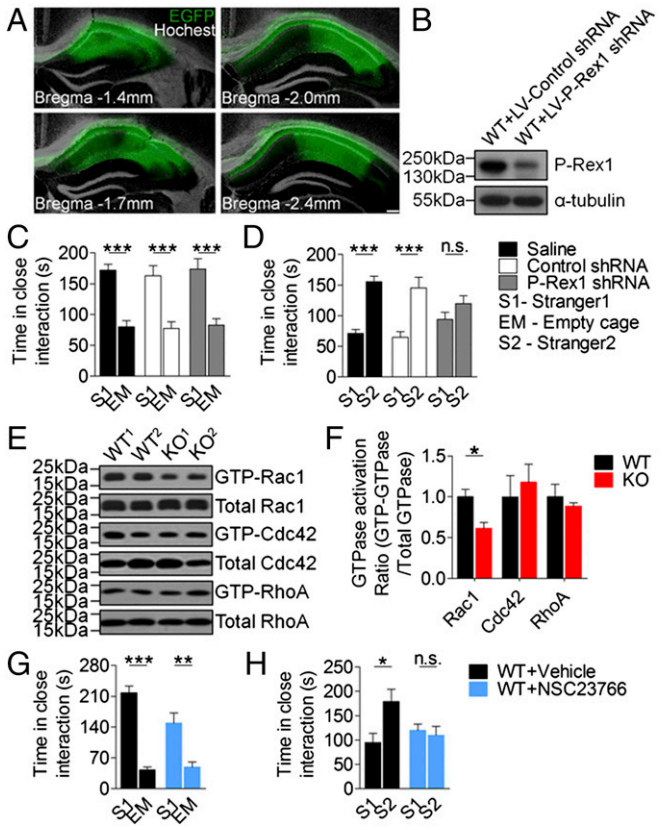

Fig. 4. P-Rex1–Rac1 signaling in the CA1 region of the hippocampus plays a vital role in social recognition behavior. (*A*) LV carrying GFP was injected into the CA1 region of 3-wk-old mice and was observed after 3 wk. The GFP was expressed in different coronal sections of the hippocampus limited to the CA1 region. (*B*) Western blot showing knockdown of endogenous P-Rex1 by LV-mediated shRNA injection in the CA1 region. (*C* and *D*) The social recognition test was performed 3 wk after LV injection. (*C*) In the sociability trial, mice injected with saline, control shRNA, or P-Rex1 shRNA spent more time in close interaction with the social partner (stranger 1, S1) than in the empty cage (EM). (*D*) In the social novelty preference trial, mice injected with P-Rex1 shRNA did not display a preference for the novel social partner (stranger 2, S2) as compared with the saline or control shRNA group ($n = 10$ mice per group). (*E* and *F*) The level of Rac1 activity (GTP-Rac1 divided by total Rac1), but not Cdc42 or RhoA, was decreased significantly in the hippocampi of *Prex1*$^{-/-}$ mice. (*G* and *H*) Mice were injected with vehicle or with the Rac1 inhibitor NSC23766. (*G*) Both groups performed normally in the sociability trial. (*H*) In the social novelty preference trial the mice injected with NSC23766 spent almost equal time in close interaction with stranger 1 and stranger 2 ($n = 9$ mice per group). *$P < 0.05$, **$P < 0.01$, ***$P < 0.001$ (two-tailed Student's *t* test or two-way ANOVA). n.s., no significance. Data are presented as mean ± SEM.

of 6-wk-old WT mice 30 min before the three-chamber test to verify further the effects of low Rac1 activation level on social recognition behavior (Fig. S5*A*). Compared with the vehicle (saline)-injected group, the mice injected with NSC23766 spent significantly less time with stranger 2 (Fig. 4 *G* and *H*), a pattern that mimicked the social recognition impairment in *Prex1*$^{-/-}$ mice and indicated that Rac1 activation in the hippocampus is involved in P-Rex1–mediated social recognition.

NMDAR-Dependent LTD Is Selectively Impaired in *Prex1*$^{-/-}$ Mice. To evaluate the synaptic localization of P-Rex1, we prepared subcellular fractions from the hippocampi of WT mice. P-Rex1 was detected not only in the synaptic vesicle (SV) fraction but also in the postsynaptic density (PSD) fraction, which was immunonegative for synaptophysin (Fig. S2*H*). This result indicates that P-Rex1 is enriched in the PSD fraction and may offer some clues as to its specific role in synaptic function.

To identify the cellular excitability and basal transmission features, we measured baseline synaptic properties at SC–CA1 synapses. We found that the intrinsic neuronal excitability did not differ between WT and *Prex1*$^{-/-}$ mice (Fig. S6 *A*–*H*). The basal excitatory transmissions, such as input–output, paired-pulse ratio, and miniature excitatory postsynaptic currents (mEPSCs), were indistinguishable between WT and *Prex1*$^{-/-}$ mice (Fig. 6 *A*–*C*), indicating that genetically deleting P-Rex1 did not affect AMPAR-mediated basal synaptic transmission and presynaptic transmitter release. We then probed the NMDAR/AMPAR ratio and found it was unaltered in *Prex1*$^{-/-}$ mice (Fig. 6*D*), suggesting that P-Rex1 ablation did not affect the equilibrium between NMDAR and AMPAR components.

We sought to investigate the physiological role of P-Rex1 in hippocampal synaptic plasticity. We examined various synaptic

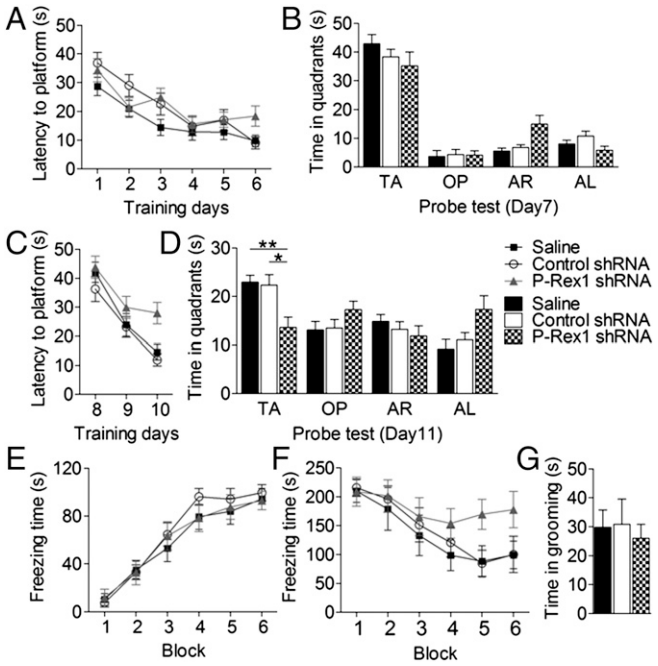

Fig. 5. Knockdown of P-Rex1 in the CA1 region of the hippocampus impairs reversal learning in the MWM (*A*–*D*) and fear extinction tests (*E* and *F*) but does not lead to repetitive grooming (*G*). (*A*–*D*) MWM test. (*A* and *B*) Learning. (*A*) Latency to locate a hidden platform (up to 60 s) decreased significantly across 7 d of training in the three groups of mice injected with saline, control shRNA, or P-Rex1 shRNA. (*B*) Probe test with the platform removed. Note that all three groups spent significantly more time in the target quadrant during a 60-s period. (*C* and *D*) Reversal learning. (*C*) Mice injected with P-Rex1 shRNA showed impairment in learning the new location of the platform across the subsequent 3 d of reversal training (the platform was switched to the opposite quadrant) as compared with the groups injected with saline or control shRNA. (*D*) Reversal probe test. Note that mice injected with saline or control shRNA, but not mice injected with P-Rex1 shRNA, spent significantly more time in the new target quadrant ($n = 9$ saline-injected mice; $n = 8$ control shRNA-injected mice; $n = 9$ P-Rex1 shRNA-injected mice). (*E*) Freezing time was increased significantly in the saline-, control shRNA-, and P-Rex1 shRNA-injected groups after one unconditional stimulus per 2-min block in a 12-min learning period consisting of six blocks. (*F*) Fear extinction was at least partially impaired in the group injected with P-Rex1 shRNA as compared with the groups injected with saline or control shRNA during a 30-min extinction period (5 min per block) 24 h after learning ($n = 10$ saline-injected mice; $n = 10$ control shRNA-injected mice; $n = 11$ P-Rex1 shRNA-injected mice). (*G*) Stereotypical grooming was similar in all three groups ($n = 10$ mice per group). (Two-tailed Student's *t* test, one-way ANOVA, or repeated-measures two-way ANOVA with genotype and treatment as independent variables). n.s., no significance. Data are presented as mean ± SEM.

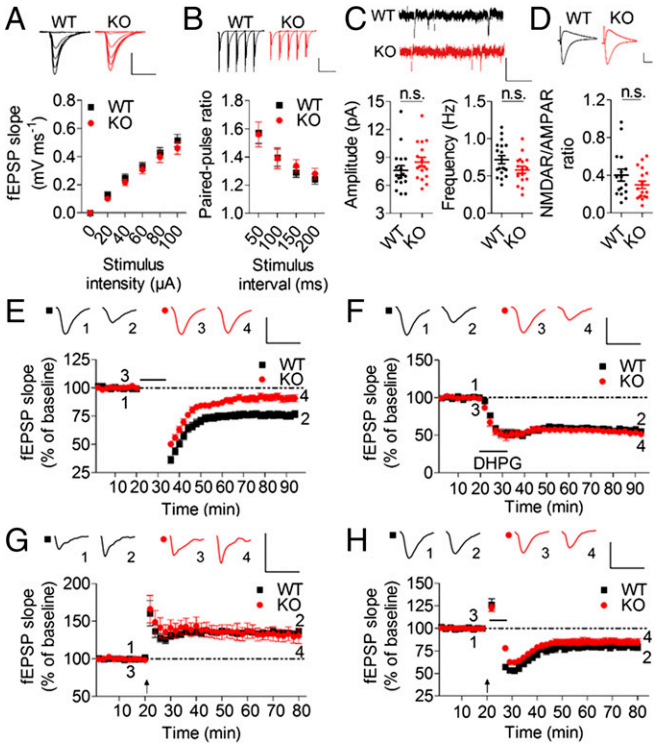

Fig. 6. Impaired NMDAR-dependent LTD in *Prex1*$^{-/-}$ mice. (*A*) Normal input–output curve at hippocampal SC–CA1 synapses (n = 6 slices per genotype). Representative voltage traces are shown at the top of each panel. n.s., no significance. [Scale bars, 1 mV (vertical) and 20 ms (horizontal).] (*B*) Normal paired-pulse ratio (n = 6 slices per genotype). [Scale bars, 0.5 mV (vertical) and 100 ms (horizontal).] (*C*) Normal mESPCs (n = 18 cells per genotype). [Scale bars, 10 pA (vertical) and 1.0 s (horizontal).] (*D*) Normal NMDAR/AMPAR ratio (n = 16 WT cells; n = 17 KO cells). [Scale bars, 100 pA (vertical) and 20 ms (horizontal).] (*E*) Impaired NMDAR LTD (n = 13 slices per genotype). (*F*) Normal mGluR LTD (n = 11 slices per genotype). (*G*) Normal LTP (n = 15 WT slices; n = 14 KO slices). (*H*) Normal depotentiation (n = 7 slices per genotype). [Scale bars in *E*–*H*, 1 mV (vertical) and 20 ms (horizontal).] (Two-tailed Student's t test or repeated-measures two-way ANOVA.) Data are presented as mean ± SEM.

plasticity models; most notably, NMDAR-dependent LTD, which can be blocked by D-(-)-2-Amino-5-phosphonopentanoic acid (D-APV) (Fig. S6*I*), was impaired in *Prex1*$^{-/-}$ mice (Fig. 6*E*). We then examined other forms of synaptic depression and found that metabotropic glutamate receptor (mGluR)-dependent LTD, was normal in *Prex1*$^{-/-}$ mice (Fig. 6*F*), suggesting that P-Rex1 is not associated with all forms of synaptic depression. We also found that long-term potentiation (LTP) (100 Hz, three strains) and depotentiation were intact in *Prex1*$^{-/-}$ mice (Fig. 6 *G* and *H*). The NMDAR-dependent LTD in primary visual cortex is not impaired in *Prex1*$^{-/-}$ mice (Fig. S6*J*), although the LTD in cerebellum is affected (Fig. S6*K*). These results indicate that P-Rex1 at SC–CA1 synapses is specifically necessary for NMDAR-dependent LTD.

PP1α Interaction with P-Rex1 and P-Rex1–Mediated Rac1 Activation Are Essential for NMDA-Induced AMPAR Endocytosis. Because NMDAR- and AMPAR-associated signaling regulates various aspects of synaptic plasticity, we tested presynaptic and postsynaptic protein expression in the total lysate and crude synaptosomal fraction (P2) from WT and *Prex1*$^{-/-}$ hippocampi but did not detect any significant differences (Fig. S7).

Rac1 was reported to be linked to NMDAR-dependent LTD (26–28). We found that Rac1 activity was increased in the slices from the CA1 region of the hippocampi s of WT mice but not in the slices from *Prex1*$^{-/-}$ mice during NMDA-induced chemical LTD (Fig. S8*A*). In contrast, we did not detect any difference in GluR1 Ser845 dephosphorylation, which is involved in hippocampal NMDAR-dependent LTD (29), between WT and *Prex1*$^{-/-}$ mice after NMDA treatment (Fig. S8*B*).

Endocytosis of AMPARs is thought to be important in the expression of LTD triggered by NMDAR activation (30). PP1 is a vital factor required for CA1 NMDAR-dependent LTD and AMPAR endocytosis (31, 32). Previous findings have suggested that PP1α, the catalytic subunit of PP1, binds to the RVxF motif in the C-terminal IP4P domain of P-Rex1 and dephosphorylates adjacent serine residues in nonneuronal cells. This effect releases steric inhibition of the DH/PH tandem domain of P-Rex1 by its IP4P domain, inducing higher basal activity of its N-terminal Rac1 guanine-nucleotide exchange function (33). Thus, we hypothesized that the NMDAR activation-induced association of PP1α with P-Rex1 is essential for NMDA-induced AMPAR endocytosis. First, we examined whether NMDA treatment induces the interaction of PP1α with P-Rex1 in slices from the CA1 region by using a coimmunoprecipitation assay. We found P-Rex1 coimmunoprecipitation with PP1α was increased with NMDA treatment (Fig. 7 *A* and *B*).

Then we expressed the GluR2 subunit tagged with HA at its extracellular N terminus in cultured hippocampal neurons. In agreement with previous reports (30, 32), we found that the surface HA-GluR2 decreased rapidly following NMDA stimulation in WT but not in *Prex1*$^{-/-}$ neurons (Fig. 7 *C* and *D*). When P-Rex1-WT was overexpressed in *Prex1*$^{-/-}$ neurons, the NMDA-induced reduction of surface AMPARs was normalized (Fig. 7*E*). Similarly, the overexpression of Rac1-WT recovered AMPAR endocytosis (Fig. 7*F*). In contrast, overexpression of P-Rex1-VAFA, a mutated form of P-Rex1 with two amino acid substitutions (V1147A/F1149A) in the RVxF motif, the loss of the binding site with PP1α (33), or P-Rex1-DHdead, a mutant with two amino acid substitutions (E56A/N238A) in the DH domain of P-Rex1, and the loss of the GEF function (34) all failed to rescue the NMDA-induced AMPAR endocytosis (Fig. 7 *G* and *H*). These results suggest that interaction of PP1α with P-Rex1 and P-Rex1–mediated Rac1 activation play crucial roles in NMDA-induced AMPAR endocytosis in hippocampal neurons (Fig. 7*I*). A model for AMPAR endocytosis mediated by the PP1–P-Rex1–Rac1 signaling pathway during NMDAR-dependent LTD induction is shown in Fig. 7*J*.

Recovery of NMDAR-Dependent LTD Impairment and Social Recognition in *Prex1*$^{-/-}$ Mice. To substantiate further the involvement of P-Rex1 in NMDAR-dependent LTD and social recognition behavior, we determined whether overexpressing WT P-Rex1 protein in pyramidal neurons of the CA1 region at postnatal day 21 would be sufficient to prevent LTD impairment and social recognition disruption in *Prex1*$^{-/-}$ mice. We found that P-Rex1 expression could be restored efficiently in the CA1 region of *Prex1*$^{-/-}$ mice (Fig. S5*B*) and that NMDAR-dependent LTD was restored fully in the group overexpressing P-Rex1 (Fig. 8*A*). In addition, P-Rex1 overexpression in the CA1 region rescued social recognition (Fig. 8 *B* and *C*) and behavioral inflexibility but not repetitive grooming (Fig. 9 *A*–*G*) in *Prex1*$^{-/-}$ mice.

Because Rac1 activation in the CA1 region was involved in P-Rex1–mediated NMDAR-dependent LTD and social recognition behavior, we asked whether overexpressed WT Rac1 in pyramidal neurons of the CA1 region could normalize LTD impairment and social recognition (Fig. S5*C*). As with P-Rex1 overexpression, we observed that overexpression of WT Rac1 fully restored NMDAR-dependent LTD impairment (Fig. 8*D*) and at least partially augmented social recognition in *Prex1*$^{-/-}$ mice (Fig. 8 *E* and *F*). Injection of Rac activator into the CA1 region also partially normalized social recognition in *Prex1*$^{-/-}$ mice (Fig. S5 *D*–*H*). Moreover, the behavioral inflexibility (but not repetitive grooming) was restored by WT Rac1 overexpression (Fig. 9 *H*–*N*).

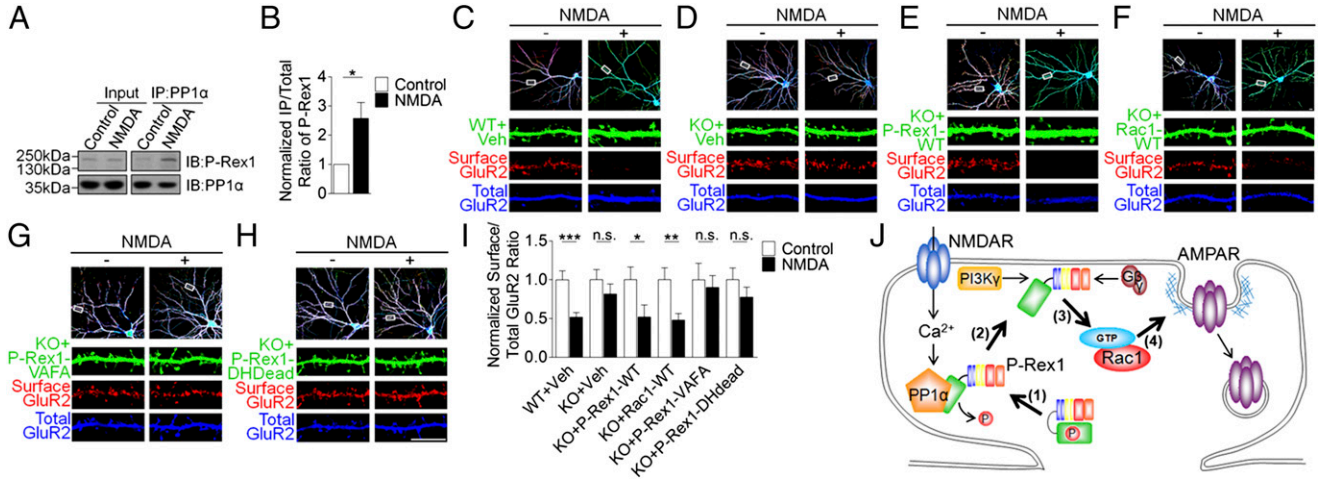

Fig. 7. Interaction of PP1α with P-Rex1 and P-Rex1–mediated Rac1 activation are essential for NMDA-induced AMPAR endocytosis. (*A*) Coimmunoprecipitation of PP1α with P-Rex1 in hippocampal slices from the CA1 region treated acutely with 100 μM NMDA. (*B*) Quantification of the NMDA-induced interaction of P-Rex1 with PP1α from five independent experiments. The ratio in the WT group was defined as 1.0. (*C*–*I*) Hippocampal neurons expressing pCAGGS-IRES-EGFP (Veh) vector (*C* and *D*), WT P-Rex1 (P-Rex1-WT) (*E*), WT Rac1 (Rac1-WT) (*F*), P-Rex1 with the VAFA mutation (P-Rex1-VAFA) (*G*), and P-Rex1 with the GEF domain dead mutation (P-Rex1-DH dead) (*H*) were treated with 50 μM NMDA for 10 min and stained for surface HA-GluR2 (red). After Triton X-100 treatment, the neurons were stained for the total HA-GluR2 (blue). The dendritic regions marked by white squares are magnified in the bottom panels. (Scale bars, 10 μm.) (*I*) Quantification of the NMDA-induced endocytosis of surface GluR2. Data are presented as the ratio of the intensity of surface staining HA-GluR2 to the intensity of total HA-GluR2 staining. The ratio in control neurons was defined as 1.0. (WT+Veh: $n = 12$ in the control group and $n = 12$ in the NMDA group; KO+Veh: $n = 12$ in the control group and $n = 14$ in the NMDA group; KO+P-Rex1 WT: $n = 10$ in the control group and $n = 11$ in the NMDA group; KO+Rac1 WT: $n = 11$ in the control group and $n = 12$ in the NMDA group; KO+P-Rex1 VAFA: $n = 10$ in the control group and $n = 11$ in the NMDA group; KO+P-Rex1 DHdead: $n = 12$ in the control group and $n = 13$ in the NMDA group). $^{*}P < 0.05$, $^{**}P < 0.01$, $^{***}P < 0.001$ (two-tailed Student's *t*-test). n.s., no significance. Data are presented as mean ± SEM. (*J*) Proposed model for AMPAR endocytosis mediated by the PP1α–P-Rex1–Rac1 signaling pathway during NMDA-LTD induction. (1) Activity-induced Ca^{2+} influx through NMDAR dephosphorylates P-Rex1 by activating PP1α. (2) Dephosphorylated P-Rex1 is recruited to membrane and activated further. (3) Active P-Rex1 catalyzes guanine–nucleotide exchange on Rac1 for GTP activation. (4) Rac1-GTP participates in actin cytoskeletal remodeling, which is essential for AMPAR endocytosis.

To explore further the association between NMDAR-dependent LTD impairment and the social recognition deficit in *Prex1*$^{-/-}$ mice, we used D-serine, a coagonist of the glycine modulatory sites on the NMDAR. We wondered whether D-serine would affect *Prex1*$^{-/-}$ NMDAR-dependent LTD impairment and the social recognition deficit. We found that D-serine fully rescued the

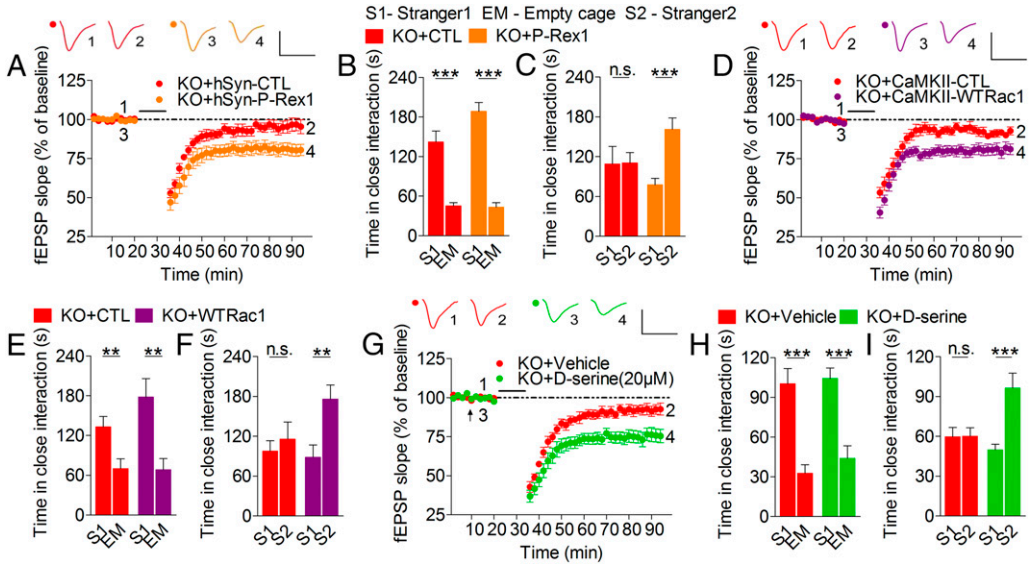

Fig. 8. Recovery of NMDAR-dependent LTD impairment and social recognition in *Prex1*$^{-/-}$ mice. (*A*) Recovery of NMDAR-dependent LTD in *Prex1*$^{-/-}$ (KO) mice by WT P-Rex1 overexpression in the pyramidal neurons of the CA1 region ($n = 8$ slices per group). (*B* and *C*) P-Rex1 overexpression clearly augmented social recognition in KO mice ($n = 8$ mice per group). (*D*) Overexpression of WT Rac1 restored the impaired NMDAR-dependent LTD in KO mice ($n = 6$ control slices; $n = 8$ WT Rac1slices). (*E* and *F*) Overexpression of WT Rac1 resulted in a clear augmentation of social recognition in KO mice ($n = 10$ control mice; $n = 12$ WT Rac1 mice). (*G*) D-serine (20 μM) restored the impaired NMDAR-dependent LTD in KO mice ($n = 7$ slices from vehicle-treated mice; $n = 8$ slices from D-serine–treated mice). (*H* and *I*) KO mice treated with D-serine (0.8 g/kg i.p.) showed improved social recognition in the three-chamber assay ($n = 8$ mice per group). [Scale bars, 1 mV (vertical) and 20 ms (horizontal) in *A*, *D*, and *G*.] $^{**}P < 0.01$, $^{***}P < 0.001$ (two-tailed Student's *t*-test and/or repeated-measures two-way ANOVA). n.s., no significance. Data are presented as mean ± SEM. CTL, control.

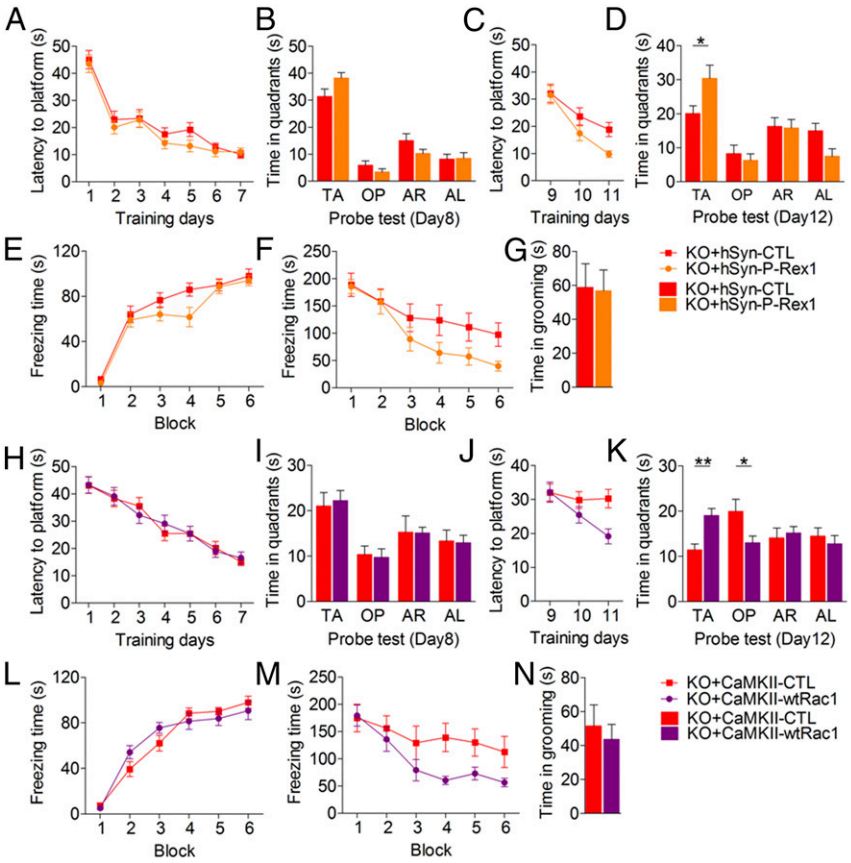

Fig. 9. Recovery of reversal learning in the MWM and fear extinction but not repetitive grooming in *Prex1*$^{-/-}$ mice. (*A*) Overexpression of WT P-Rex1 made no difference in the latency in locating a hidden platform across 7 d of training compared with control group. (*B*) Probe test. Note that overexpression of WT P-Rex1 resulted in almost identical time spent in the target quadrant compared with control group. (*C*) WT P-Rex1 overexpression resulted in a clear augmentation of reversal learning in KO mice because they required less time to reach the new location of the hidden platform. (*D*) Reversal probe test. Note that group with WT P-Rex1 overexpression spent significantly more time in the new target quadrant ($n = 11$ in the KO+CTL group; $n = 10$ in the KO+WT P-Rex1 group). (*E*) Freezing time was increased significantly after one unconditional stimulus per block in both WT P-Rex1 and control groups. (*F*) Freezing time was decreased more significantly in the group overexpressing WT P-Rex1 than in the control group 24 h after learning ($n = 13$ mice per group). (*G*) Stereotypical grooming was not significantly different between the group overexpressing WT P-Rex1 and the control group ($n = 9$ mice per group). (*H*) Overexpression of WT Rac1 made no difference in the latency in locating a hidden platform across 7 d of training compared with the control group. (*I*) Probe test. Note that overexpression of WT Rac1 led to almost identical time spent in the target quadrant compared with the control group. (*J*) WT Rac1 overexpression resulted in a clear augmentation of reversal learning in KO mice because they required less time to reach the new location of the platform. (*K*) Reversal probe test. Note that the group overexpressing WT Rac1 spent significantly more time than the control group in the new target quadrant ($n = 12$ for the KO+CTL group; $n = 11$ for the KO+WT Rac1 group). (*L*) Freezing time was increased significantly in both the WT Rac1 and control groups after one unconditional stimulus per block. (*M*) Freezing time was decreased more significantly in the group overexpressing WT Rac1 than in the control group 24 h after conditioning to the stimulus ($n = 11$ mice per group). (*N*) Stereotypical grooming was not significantly different between the group overexpressing WT Rac1 and the control group ($n = 10$ mice per group). $^{*}P < 0.05$, $^{**}P < 0.01$ (two-tailed Student's *t*-test or repeated-measures two-way ANOVA with genotype and treatment as independent variables). n.s., no significance. Data are presented as mean ± SEM.

NMDAR-dependent LTD impairment at *Prex1*$^{-/-}$ SC–CA1 synapses (Fig. 8*G*) and significantly improved social recognition (Fig. 8 *H* and *I*). These results confirmed postsynaptic PP1α–P-Rex1–Rac1 signaling and its direct involvement in hippocampal NMDAR-dependent LTD and social recognition behavior.

Discussion

LTD is regarded as a critical form of synaptic plasticity involving the modification or elimination of previously learned information (35). Although pharmacological or genetic disruption of NMDAR-dependent LTD in the CA1 region is related to impairments in behavioral flexibility (23–25), the mechanism underlying the role of NMDAR-dependent synaptic plasticity in social recognition is not fully understood. Here we used *Prex1*$^{-/-}$ mice and found a tight link between NMDAR-dependent LTD in the CA1 region and behavioral phenotypes including social recognition, reversal learning of spatial memory, and extinction training of contextual fear memory but found no correlation with repetitive grooming or with the delayed nonmatch to place T-maze task. Our findings may indicate that reversal learning of the memories (such as spatial memory and contextual fear memory) and correct choices in the delayed nonmatch to place T-maze task reflect different aspects of cognitive functions (23). We believed that not only social memory but also other cognitive functions are impaired in *Prex1*$^{-/-}$ mice, possibly because of abnormal LTD, suggesting unique characteristics of cognitive dysfunction in *Prex1*$^{-/-}$ mice.

In addition to the CA1 region of the hippocampus, P-Rex1 is highly expressed in the pyramidal neurons of the superficial layer of cortex. However, the NMDAR-dependent LTD in primary visual cortex was not affected in *Prex1*$^{-/-}$ mice, indicating that, to some extent, P-Rex1 has a specific role in NMDAR-dependent LTD in the CA1 region.

The molecular mechanism for NMDAR-dependent LTD induction is not fully understood. We found that NMDA triggered the interaction between PP1α and P-Rex1 that activated Rac1, which is critical for AMPAR endocytosis and LTD expression. These results implicate an essential role of PP1α–P-Rex1–Rac1 signaling in NMDAR-dependent LTD in the CA1 region.

In conclusion, our results provide the first report, to our knowledge, of a genetic association of P-Rex1 and its copy number deletion with ASDs, the role of P-Rex1 in hippocampal synaptic plasticity and autism-like behaviors, a pivotal role in the induction of NMDAR-dependent LTD in the CA1 region, and AMPAR endocytosis via a postsynaptic PP1α–P-Rex1–Rac1 signaling pathway. Our findings suggested that P-Rex1 might be a previously unreported target for therapeutic approaches to treat disorders with symptoms of social deficit and/or cognitive dysfunction such as ASDs.

Materials and Methods

Further details are provided in *SI Materials and Methods*.

Subjects. For the family-based genetic association study, 239 Chinese Han family trios (singleton autistic disorder patients and their unaffected

biological parents) were recruited for the present study at the Institute of Mental Health, Peking University, Beijing. Of the 239 autistic child probands, 226 were male, and 13 were female. The mean age of the children at the time of testing was 7.5 y. Diagnoses of autism were established by two senior psychiatrists. All patients fulfilled the *Diagnostic and Statistical Manual of Mental Disorders*, Fourth Edition (DSM-IV) criteria for autistic disorder. To assess the cases, the Childhood Autism Rating Scale (36) and Autism Behavior Checklist (37) were used. Children with phenylketonuria, fragile X syndrome, tuberous sclerosis, or a previously identified chromosomal abnormality were excluded. To decrease the heterogeneity of the cases, children affected with Asperger disorder and Rett syndrome were excluded from our study. For analysis of copy number variants, 227 unrelated healthy controls were recruited from the community by advertisements during physical examinations. Psychiatrists performed a simple, nonstructured interview to exclude individuals with a history of mental health and neurological diseases. Similarly, for P-Rex1 mRNA analysis in peripheral blood cells, blood was collected from 24 male autistic patients and 25 age-matched healthy male controls. All participants in this study provided written informed consent. Written informed consents for children were obtained from their legal guardians. This study was approved by the Ethics Committee of the Institute of Mental Health, Peking University. Genetic association and copy number variants analysis protocols are provided in *SI Materials and Methods*.

Mouse Strains. The *Prex1*$^{-/-}$ mice in the C57BL6 background were a kind gift from Heidi Welch, The Babraham Institute, Cambridge, UK (10). Generation of this knockout line was described previously (9).

Animal Experiments. Animals were housed at a constant temperature of 25 °C in a 12-h/12-h light/dark cycle (lights off at 20:00), with food and water available ad libitum. Three to five mice were housed per cage by genotype. Only aged-matched male mice were used for behavioral experiments. All animal experimental procedures were reviewed and approved by the Peking University Institutional Animal Care and Use Committee and the Peking University Committee on Animal Cares. Details on animal behavioral tests are provided in *SI Materials and Methods*.

Electrophysiology. Animals were killed, and hippocampal coronal slices (350 μm) were obtained using a vibratome (Leica VT 1000S). Field excitatory postsynaptic potentials (fEPSPs) in the CA1 region of the hippocampus were recorded. The recording electrode was placed ∼400 μm away from the stimulating electrode in the stratum radium of the CA1 region. All data were recorded using pCLAMP 10 software (Molecular Devices). The fEPSPs, NMDA/AMPA ratio, and action potentials were analyzed by Clampfit 10 software (Molecular Devices). The mEPSCs were analyzed using Mini Analysis software (Synaptosoft).

Rac1, Cdc42, and RhoA-GTP Assays. Individual 6-wk-old mouse hippocampi were homogenized with a glass homogenizer in 1 mL of cold 1× MLB lysis buffer [25 mM Hepes (pH 7.5), 150 mM NaCl, 1% (vol/vol) IGEPAL CA-630, 10 mM MgCl2, 1 mM EDTA, and 2% (vol/vol) glycerol] to which protease inhibitor mixture (Roche Diagnostics Ltd.) and phosphatase inhibitor mixture (Roche) were added. The lysate was centrifuged at 12,000 × *g* for 20 min at 4 °C. The supernatant was incubated with 10 μg of GST-PAK-BD (for Rac1 and Cdc42) (Millipore) or GST-Rhotekin (for RhoA) (Millipore) fusion protein bound to glutathione-coupled Sepharose beads for 45 min at 4 °C. Beads were washed three times in the lysis buffer, and bound proteins were eluted in loading buffer and subjected to SDS/PAGE gel. Proteins were transferred electrophoretically to nitrocellulose, and the filters were incubated with antibodies. In all cases, 5% of the initial homogenate input for the pull-down assay was electrophoresed and probed with antibody, and activated levels were normalized to the total input levels of Rac1, Cdc42, or RhoA.

Statistical Analysis. Experimenters were blinded to the genotype during testing and scoring. All data are presented as mean ± SEM. Statistical analyses were performed using SPSS 16.0 (SPSS), and details of the results are summarized in Dataset S1. Statistical significance was set a priori at 0.05.

ACKNOWLEDGMENTS. We thank Prof. Heidi Welch for providing the mouse model and P-Rex1 plasmids and Prof. Michisuke Yuzaki for providing the HA-GluR2 plasmid. This work was supported by Grants 2010CB833905 and 2013CB835103 from Program 973 of the Ministry of Science and Technology of China; by Grants 91232305, 81471360, 81222017, 81471383, 81221002, and 81501183 from the National Natural Science Foundation of China; and by Shenzhen Basic Research Grant JC201104220331A.

1. Volkmar FR, Pauls D (2003) Autism. *Lancet* 362(9390):1133–1141.
2. O'Hearn K, Schroer E, Minshew N, Luna B (2010) Lack of developmental improvement on a face memory task during adolescence in autism. *Neuropsychologia* 48(13):3955–3960.
3. D'Cruz AM, et al. (2013) Reduced behavioral flexibility in autism spectrum disorders. *Neuropsychology* 27(2):152–160.
4. Yasuda Y, et al. (2014) Cognitive inflexibility in Japanese adolescents and adults with autism spectrum disorders. *World J Psychiatry* 4(2):42–48.
5. Abrahams BS, Geschwind DH (2008) Advances in autism genetics: On the threshold of a new neurobiology. *Nat Rev Genet* 9(5):341–355.
6. Shishido E, Aleksic B, Ozaki N (2014) Copy-number variation in the pathogenesis of autism spectrum disorder. *Psychiatry Clin Neurosci* 68(2):85–95.
7. Bourgeron T (2009) A synaptic trek to autism. *Curr Opin Neurobiol* 19(2):231–234.
8. Welch HCE, et al. (2002) P-Rex1, a PtdIns(3,4,5)P3- and Gbetagamma-regulated guanine-nucleotide exchange factor for Rac. *Cell* 108(6):809–821.
9. Welch HCE, et al. (2005) P-Rex1 regulates neutrophil function. *Curr Biol* 15(20):1867–1873.
10. Lindsay CR, et al. (2011) P-Rex1 is required for efficient melanoblast migration and melanoma metastasis. *Nat Commun* 2:555.
11. Yoshizawa M, et al. (2005) Involvement of a Rac activator,P-Rex1, in neurotrophin-derived signaling and neuronal migration. *J Neurosci* 25(17):4406–4419.
12. Waters JE, et al. (2008) P-Rex1 - a multidomain protein that regulates neurite differentiation. *J Cell Sci* 121(Pt 17):2892–2903.
13. Alter MD, et al. (2011) Autism and increased paternal age related changes in global levels of gene expression regulation. *PLoS One* 6(2):e16715.
14. Silverman JL, Yang M, Lord C, Crawley JN (2010) Behavioural phenotyping assays for mouse models of autism. *Nat Rev Neurosci* 11(7):490–502.
15. Moy SS, et al. (2004) Sociability and preference for social novelty in five inbred strains: An approach to assess autistic-like behavior in mice. *Genes Brain Behav* 3(5):287–302.
16. Hitti FL, Siegelbaum SA (2014) The hippocampal CA2 region is essential for social memory. *Nature* 508(7494):88–92.
17. Yang L, et al. (2013) Hypocretin/orexin neurons contribute to hippocampus-dependent social memory and synaptic plasticity in mice. *J Neurosci* 33(12):5275–5284.
18. Thor DH, Holloway WR (1982) Social memory of the male laboratory rat. *J Comp Physiol Psychol* 96(6):1000–1006.
19. Ferguson JN, et al. (2000) Social amnesia in mice lacking the oxytocin gene. *Nat Genet* 25(3):284–288.
20. Crawley JN (2007) Mouse behavioral assays relevant to the symptoms of autism. *Brain Pathol* 17(4):448–459.
21. Donald S, et al. (2008) P-Rex2 regulates Purkinje cell dendrite morphology and motor coordination. *Proc Natl Acad Sci USA* 105(11):4483–4488.
22. Kogan JH, Frankland PW, Silva AJ (2000) Long-term memory underlying hippocampus-dependent social recognition in mice. *Hippocampus* 10(1):47–56.
23. Nicholls RE, et al. (2008) Transgenic mice lacking NMDAR-dependent LTD exhibit deficits in behavioral flexibility. *Neuron* 58(1):104–117.
24. Kim JI, et al. (2011) PI3Kγ is required for NMDA receptor-dependent long-term depression and behavioral flexibility. *Nat Neurosci* 14(11):1447–1454.
25. Dong Z, et al. (2013) Hippocampal long-term depression mediates spatial reversal learning in the Morris water maze. *Neuropharmacology* 64:65–73.
26. Bongmba OYN, Martinez LA, Elhardt ME, Butler K, Tejada-Simon MV (2011) Modulation of dendritic spines and synaptic function by Rac1: A possible link to Fragile X syndrome pathology. *Brain Res* 1399:79–95.
27. Martinez LA, Tejada-Simon MV (2011) Pharmacological inactivation of the small GTPase Rac1 impairs long-term plasticity in the mouse hippocampus. *Neuropharmacology* 61(1-2):305–312.
28. Benoist M, et al. (2013) MAP1B-dependent Rac activation is required for AMPA receptor endocytosis during long-term depression. *EMBO J* 32(16):2287–2299.
29. Lee HK, Kameyama K, Huganir RL, Bear MF (1998) NMDA induces long-term synaptic depression and dephosphorylation of the GluR1 subunit of AMPA receptors in hippocampus. *Neuron* 21(5):1151–1162.
30. Beattie EC, et al. (2000) Regulation of AMPA receptor endocytosis by a signaling mechanism shared with LTD. *Nat Neurosci* 3(12):1291–1300.
31. Morishita W, et al. (2001) Regulation of synaptic strength by protein phosphatase 1. *Neuron* 32(6):1133–1148.
32. Unoki T, et al. (2012) NMDA receptor-mediated PIP5K activation to produce $PI(4,5)P_2$ is essential for AMPA receptor endocytosis during LTD. *Neuron* 73(1):135–148.
33. Barber MA, et al. (2012) The guanine-nucleotide-exchange factor P-Rex1 is activated by protein phosphatase 1α. *Biochem J* 443(1):173–183.
34. Hill K, et al. (2005) Regulation of P-Rex1 by phosphatidylinositol (3,4,5)-trisphosphate and Gbetagamma subunits. *J Biol Chem* 280(6):4166–4173.
35. Collingridge GL, Peineau S, Howland JG, Wang YT (2010) Long-term depression in the CNS. *Nat Rev Neurosci* 11(7):459–473.
36. Schopler E, Reichler RJ, DeVellis RF, Daly K (1980) Toward objective classification of childhood autism: Childhood Autism Rating Scale (CARS). *J Autism Dev Disord* 10(1):91–103.
37. Krug DA, Arick J, Almond P (1980) Behavior checklist for identifying severely handicapped individuals with high levels of autistic behavior. *J Child Psychol Psychiatry* 21(3):221–229.
38. Jurinke C, van den Boom D, Cantor CR, Köster H (2002) The use of MassARRAY technology for high throughput genotyping. *Adv Biochem Eng Biotechnol* 77:57–74.
39. Storm N, Darnhofer-Patel B, van den Boom D, Rodi CP (2003) MALDI-TOF mass spectrometry-based SNP genotyping. *Methods Mol Biol* 212:241–262.

40. O'Connell JR, Weeks DE (1998) PedCheck: A program for identification of genotype incompatibilities in linkage analysis. *Am J Hum Genet* 63(1):259–266.
41. Rabinowitz D, Laird N (2000) A unified approach to adjusting association tests for population admixture with arbitrary pedigree structure and arbitrary missing marker information. *Hum Hered* 50(4):211–223.
42. Du R, et al. (2012) Efficient typing of copy number variations in a segmental duplication-mediated rearrangement hotspot using multiplex competitive amplification. *J Hum Genet* 57(8):545–551.
43. Liu Y, et al. (2013) Lack of association between NLGN3, NLGN4, SHANK2 and SHANK3 gene variants and autism spectrum disorder in a Chinese population. *PLoS One* 8(2): e56639.
44. Inagaki S, et al. (2001) Sema4c, a transmembrane semaphorin, interacts with a postsynaptic density protein, PSD-95. *J Biol Chem* 276(12):9174–9181.
45. Vorhees CV, Williams MT (2006) Morris water maze: Procedures for assessing spatial and related forms of learning and memory. *Nat Protoc* 1(2):848–858.
46. Dai JX, et al. (2008) Enhanced contextual fear memory in central serotonin-deficient mice. *Proc Natl Acad Sci USA* 105(33):11981–11986.
47. Ryan BC, Young NB, Crawley JN, Bodfish JW, Moy SS (2010) Social deficits, stereotypy and early emergence of repetitive behavior in the C58/J inbred mouse strain. *Behav Brain Res* 208(1):178–188.
48. Yang M, Crawley JN (2009) Simple behavioral assessment of mouse olfaction. *Curr Protoc Neurosci* Chapter 8:Unit 8:24.